PERGAMON

International Journal of Heat and Mass Transfer 43 (2000) 2541–2552

International Journal of HEAT and MASS TRANSFER

www.elsevier.com/locate/ijhmt

Heat transfer coefficient at the metal–mould interface in the unidirectional solidification of Cu–8%Sn alloys

M.A. Martorano, J.D.T. Capocchi*

Department of Metallurgical and Materials Engineering, Polytechnic School, University of São Paulo, Av. Prof. Mello Moraes, 2463, CEP 05508-900 São Paulo, SP, Brazil

Received 2 March 1999; received in revised form 17 September 1999

Abstract

The heat transfer coefficient at the metal–mould interface of a unidirectional solidification system was calculated by an algorithm that uses the whole domain method for the inverse solution to the heat conduction differential equation with phase change. Experimental curves of temperature as a function of time, collected during solidification of Cu–8%Sn alloys subject to four different conditions, were used as input to the algorithm. Accordingly, the heat transfer coefficient at the metal–mould interface was obtained for those conditions. The estimated heat transfer coefficient values are in good agreement with the ones published in the literature. © 2000 Elsevier Science Ltd. All rights reserved.

Keywords: Heat transfer coefficient; Metal–mould interface; Inverse heat conduction problem; Directional solidification

1. Introduction

The mathematical modelling of solidification processing of metals has had a tremendous breakthrough in the past decades with the advent of personal computers. Basic phenomena such as nucleation, liquid and solid movement have been taken into account in the latest models and their results have reached increasingly good agreement with experimental evidence. Nevertheless, there are still no accepted comprehensive models dealing with the heat transfer coefficient at metal–mould interfaces by means of a first principle approach. Although inaccurate assumptions relative to this heat transfer coefficient are not expected to cause large errors in the thermal field modelling of sand castings, this is not the case for permanent mould or die castings [1].

Ho and Pehlke [1], Sharma and Krishnan [2] and Chiesa [3] have studied the heat transfer at the interface between cast metals and metallic moulds or chills and have outlined the basic mechanisms. Frequently, there is one prevailing mechanism depending on the casting process and the time elapsed after the beginning of solidification. The relative movement of the casting and mould surfaces, initially in contact, is likely to determine the most important heat transfer mechanism. This relative movement might cause the appearance of a continuous gap or the application of pressure at the metal–mould interface. Furthermore, if coatings are applied on the mould surface, heat conduction through it must also be considered [3].

Modelling of heat transfer coefficients at metal–mould interfaces based on first principles should take account of all important heat transfer mechanisms, including prediction of gap dimensions and

* Corresponding author. Tel.: +55-11-818-5494; fax: +55-11-818-5421.

E-mail address: jdtcapoc@usp.br (J.D.T. Capocchi).

0017-9310/00/$ - see front matter
PII: S0017-9310(99)00298-7

Nomenclature

Eq	Eq. (7)
H	enthalpy
h_{M}	heat transfer coefficient between metal and copper base
h_{m}	heat transfer coefficient at the metal–insulating sleeve interface
h_{MB}	heat transfer coefficient across coating–copper base interface
h_{MC}	heat transfer coefficient across metal–water cooled interface
h_{MR}	heat transfer coefficient across metal–ceramic coating interface
h_{MW}	heat transfer coefficient between copper base and cooling water
h^*	tentative value of the heat transfer coefficient
$\hat{h}$	functional for the heat transfer coefficient
$h_1, h_2, \ldots, h_n$	components of the heat transfer coefficient h_{M}
$\vec{h}$	vector representation of $(h_1, h_2, \ldots, h_n)$
IHCP	inverse heat conduction problem
K	thermal conductivity
L	length of cylindrical cast sample
p	number of measurements recorded from one thermocouple
q	number of thermocouples used in the minimisation procedure (TM1–TM4)
qr	radiation heat flux at metal–mould interface
R_{i}	radius of cylindrical cast sample
r	radial co-ordinate
T	temperature
T_{a}	temperature of cooling water (26°C) for water-cooled base or TM7 for massive copper base
TC	temperature calculated by the heat transfer mathematical model
TM	temperature measured by thermocouples
$XhiTC$	sensitivity coefficient, Eq. (15)
t	time
z	longitudinal co-ordinate

Greek symbols

Δh	variation of the heat transfer coefficient components
Δx_{c}	coating thickness
Δx_{g}	width of an ideal gap between two surfaces
Δx_{L}	thickness of water-cooled base wall
ε	emissivity or increment used in Eq. (15)
ρ	density
σ	Stefan–Boltzmann constant

Subscripts

c	ceramic coating on massive copper base
cs	ceramic coating surface
i	index of one heat transfer coefficient component or indication of material type
k	index of one thermocouple
L	wall of water-cooled base
M	metal
m	insulating sleeve
Ms	cast sample bottom surface
n	number of unknown heat transfer coefficient components
sM	lateral surface of cylindrical cast samples
sm	inner surface of insulating sleeve
v	index of time associated with a recorded temperature measurement

pressure forces applied at the interface. Consequently, owing to these complexities, modellers have relied on empirical coefficients specific to their materials and conditions, which means that accurate empirical or semi-empirical coefficients and methods to calculate them must be available.

Beck et al. [4] have reviewed a group of methods used to solve the inverse heat conduction problem (IHCP). This problem is always present when the heat transfer coefficient or heat flux at body surfaces need to be calculated from interior temperature measurements. The whole domain estimation is one technique used to solve the IHCP and was firstly proposed by Frank [5], who worked with a linear heat conduction differential equation. In this method, after assuming a mathematical model of the heat conduction inside the body and a certain functional form of the heat flux at the surface, all the unknowns in this functional form are calculated with the help of an optimisation technique. This technique firstly assesses the effect of variations in the unknowns on the error between measured temperatures and those calculated by the assumed heat conduction model. Subsequently, it seeks to decrease the error until a minimum value is reached.

The whole domain estimation has the advantage

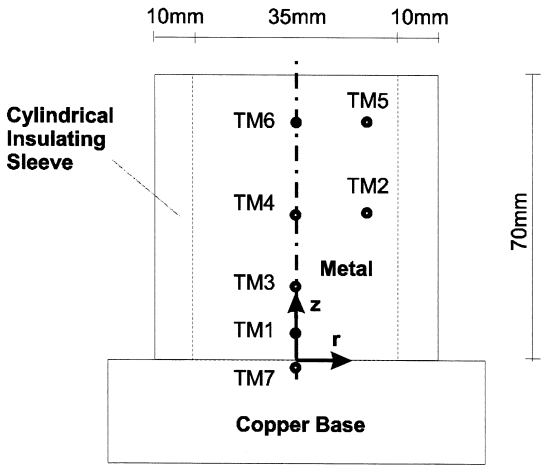

Fig. 1. Schematic view of casting system with a cylindrical cavity. TM is a thermocouple in contact with the alloy. TM7 is only present when the copper base is massive.

of being more stable than other possible inverse solution methods since all experimental temperatures are used in the computation of all unknowns. Another advantage of the whole domain estimation, usually overlooked in the literature, is the fact that only minor modifications of implemented heat transfer codes are needed to solve the equivalent IHCP problem.

Spitzer [6] applied the whole domain estimation to the solidification non-linear problem and obtained results in very good agreement with published data. In his work, the one-dimensional heat conduction equation was solved inversely by a finite difference fully implicit enthalpy method after assuming a functional form of the heat transfer coefficient at the metal–mould interface (h_M).

The present work is aimed at calculating the heat transfer coefficient at the metal–mould interface of a directional solidification system where Cu–8%Sn alloy samples were subject to four different experimental conditions usually found in metal casting with metallic moulds. Although these coefficients are essential for modelling solidification, values for this alloy and some of the experimental conditions used here were not found in the literature. The processing variables employed were selected to investigate the effect of different thermal conditions as well as different dendritic structures on the heat transfer coefficient. The mathematical model of heat conduction within the solidifying alloy used the two-dimensional heat conduction differential equation. The heat transfer coefficient at the metal–mould interface was assumed to vary linearly between unknown values at certain specific times. The whole domain estimation was employed to find those unknown values by a non-linear least square algorithm.

2. Experimental procedure

Charges of nominal composition Cu–8%Sn composed of electrolytic copper and tin were melted in an electric resistance furnace and deoxidised with Cu–15%P. The liquid alloy was cast into cylindrical shapes using the casting system shown in Fig. 1. This system consists of a cylindrical thermal insulating sleeve made of a mullite based material (Kalmin TH[1]) standing on a copper base employed to extract heat directionally.

A factorial experimental design was used to define casting conditions. Two experimental variables at two levels were identified, resulting in four different experiments, carried out in random order as shown in Table 1. The two experimental variables were named Thermal Conditions and Inoculation, both of which have two levels, as follows:

- Thermal Condition (A): Thermal conditions that favour equiaxed dendritic growth, corresponding to a pouring temperature[2] of 1110°C, and heat extraction by a massive copper base whose upper surface was covered with an insulating mullite based coating (Dycote[3] 140);
- Thermal Condition (B): Thermal conditions that favour columnar dendritic growth, corresponding to a pouring temperature of 1270°C and heat extraction through a water-cooled copper base;
- Inoculation (A): No inoculation was made;
- Inoculation (B): Cu–50%Zr was added for inoculation before pouring liquid metal into the cylindrical cavity.

As shown above, the pouring temperature and the type of copper base used to extract heat were changed simultaneously from one thermal condition level to the other. This was done to force the dendritic structure to change from columnar to equiaxed or vice versa, allowing the examination of this effect on the heat transfer coefficient.

A mullite based coating was applied by spray gun on the massive copper base surface preheated to 150°C. After application, the coating thickness was decreased to approximately 750 μm by a horizontal milling machine. The water-cooled copper base, inside which water velocity was approximately 4 m s^{-1}, had

[1] Kalmin TH is a trademark of FOSECO International Ltd.
[2] Pouring temperature is actually the temperature displayed by the furnace dial just before the crucible was removed for pouring.
[3] Dycote 140 is a trademark of FOSECO International Ltd.

its surface ground with a 600 grit emery paper before the beginning of each experiment.

Six R type thermocouples (Pt–13%Rh, Pt) were placed within the cylindrical cavity as shown in Fig. 1. Another, thermocouple (TM7) was positioned in the massive copper base, close to the metal–base interface. The thermocouples in the mould cavity were 0.35 mm in diameter and their junctions were coated with a zirconate based ceramic layer for protection against electrical and chemical interactions with the cast alloy. The total thermocouple diameter after coating never exceeded 1 mm. The thermocouples were connected to a data acquisition system that collected data at a rate of approximately eight measurements per second. More details of experiments can be found elsewhere [7].

3. Heat transfer coefficient calculation

The heat transfer coefficient between metal and copper base (h_M) and that at the metal–insulating sleeve interface (h_m) were calculated by the whole domain estimation technique. Some fixed times were previously defined along the total experiment period, and the values of h_M at such times were unknown components to be calculated by the algorithm. In between those predetermined times, h_M was considered to vary linearly, so that on computing the unknowns, h_M would be given at any instant. On the other hand, h_m was assumed to be constant throughout the experimentation.

3.1. Mathematical modelling of heat transfer

The whole domain method to solve the IHCP is a search for the least square error between measured and calculated temperatures by varying the unknown components of the heat transfer coefficient. Therefore, a mathematical model to calculate the temperature field was constructed for the unidirectional solidification system in hand. The mathematical model consisted of the heat conduction equation written for the cavity and sleeve wall in the cylindrical co-ordinate system shown in Fig. 1, resulting in the following equations:

$$\rho_i \frac{\partial H_i}{\partial t} = \frac{\partial}{\partial z}\left(K_i \frac{\partial T_i}{\partial z}\right) + \frac{1}{r}\frac{\partial}{\partial r}\left(rK_i \frac{\partial T_i}{\partial r}\right) \qquad i = \begin{cases} \text{m, sleeve} \\ \text{M, metal} \end{cases} \tag{1}$$

Initially, the liquid alloy temperature was considered to be homogeneous and its value was obtained from the temperatures measured by the thermocouples mentioned before. The metal domain was defined to the right of the z-axis due to the inherent symmetry in the temperature field, and its boundary conditions are described below:

$$K_M \frac{\partial T_M}{\partial r}(r = 0, z, t) = 0 \tag{2}$$

$$K_M \frac{\partial T_M}{\partial r}(r = R_i, z, t) = h_m(T_{sm} - T_{sM}) \tag{3}$$

$$K_M \frac{\partial T_M}{\partial z}(r, z = 0, t) = h_M(T_{sM} - T_a) \tag{4}$$

$$T_M(r, z = L, t) = f(\text{TM5, TM6}) \tag{5}$$

The boundary conditions for the insulating sleeve domain are presented elsewhere [7]. Eq. (5) is a boundary condition of Dirichlet type, i.e. the upper boundary of the metal domain is fixed exactly at TM5 and TM6 vertical position and its temperature at any time is a linear interpolation of the thermocouple measurements.

Differential equation (1) subject to the boundary and initial conditions were solved by a fully implicit finite volume technique using a rectangular mesh of 21 nodes along the z-axis, 16 nodes along the r-axis in the metal domain and further nine nodes in the insulating sleeve domain. The phase change during solidification was handled by the enthalpy method in a way similar to that presented by Shamsundar and Rooz [8]. The insulating sleeve enthalpy as a function of temperature was derived in a straightforward manner from its specific heat. The alloy enthalpy was computed for every volume element after knowing its solid and liquid fraction dependence on temperature, obtained

Table 1
Definition of the four experimental conditions to which cast samples were subject

Experimental condition	Thermal condition	Inoculation	Experiment order
Eq-Inoc	A	B	2
Eq-NoInoc	A	A	4
Col-Inoc	B	B	1
Col-NoInoc	B	A	3

by the microsegregation model proposed by Brody and Flemings [9] and corrected by Clyne and Kurz [10].

3.2. Optimisation by a least square method

The solution to the mathematical model of heat transfer described previously can be written as:

$$TC = TC(r, z, t, h_1, h_2, \ldots, h_n) \tag{6}$$

where TC is the temperature calculated at co-ordinates (r, z) and time t. The components of the coefficient h_M, defined at some specific times along the simulation period, and the coefficient h_m are all named $h_1, h_2, \ldots, h_n$. They are the unknowns to be determined. The sum of the square of the differences between calculated and measured temperatures is given by:

$$Eq(h_1, h_2, \ldots, h_n) = \sum_{k=1}^{q}\sum_{v=1}^{p}\left[TC\left(r_k, z_k, t_v, \vec{h}\right) - TM_{k,v}\right]^2 \tag{7}$$

The whole domain estimation technique is based on the hypothesis that a correct $\vec{h}$ will result in the smallest squared error given by Eq. (7). According to differential calculus, the following system of n non-linear equations must be satisfied at that least error:

$$\frac{\partial Eq(\vec{h})}{\partial h_i} = 2\sum_{k=1}^{q}\sum_{v=1}^{p}\left[TC\left(r_k, z_k, t_v, \vec{h}\right) - TM_{k,v}\right] \times \frac{\partial TC\left(r_k, z_k, t_v, \vec{h}\right)}{\partial h_i} = 0 \quad i = 1, 2, \ldots, n \tag{8}$$

The Newton–Raphson method was used to solve this system after expanding TC in a truncated Taylor series:

$$TC\left(r_k, z_k, t_v, \vec{h} + \Delta\vec{h}\right) \approx TC\left(r_k, z_k, t_v, \vec{h}\right) + \sum_{i=1}^{n}\frac{\partial TC\left(r_k, z_k, t_v, \vec{h}\right)}{\partial h_i}\Delta h_i \quad i = 1, 2, \ldots, n \tag{9}$$

where $\vec{h}$ is now a first approximation to the heat transfer coefficient components and $\Delta\vec{h}$ is a tentative correction to make these components satisfy Eq. (8). After inserting Eq. (9) in Eq. (8), written for $h + \Delta\vec{h}$, and making the approximation below [11]:

$$\frac{\partial TC\left(r_k, z_k, t_v, \vec{h} + \Delta\vec{h}\right)}{\partial h_i} \approx \frac{\partial TC\left(r_k, z_k, t_v, \vec{h}\right)}{\partial h_i} \tag{10}$$

the following system of n linear equations is derived:

$$\left(\sum_{k=1}^{q}\sum_{v=1}^{p}\frac{\partial TC_{k,v}}{\partial h_1}\frac{\partial TC_{k,v}}{\partial h_i}\right)\Delta h_1 + \left(\sum_{k=1}^{q}\sum_{v=1}^{p}\frac{\partial TC_{k,v}}{\partial h_2}\frac{\partial TC_{k,v}}{\partial h_i}\right)\Delta h_2 + \ldots + \left(\sum_{k=1}^{q}\sum_{v=1}^{p}\frac{\partial TC_{k,v}}{\partial h_n}\frac{\partial TC_{k,v}}{\partial h_i}\right)\Delta h_n = -\sum_{k=1}^{q}\sum_{v=1}^{p}\left[\left(TC_{k,v} - TM_{k,v}\right)\frac{\partial TC_{k,v}}{\partial h_i}\right] \quad i = 1, 2, \ldots, n \tag{11}$$

where $TC_{k,v}$ and all $(\partial TC_k, v)/(\partial h_i)$ coefficients were computed by the heat transfer mathematical model described earlier. The system presented above was solved for corrections $\Delta\vec{h}$ many times. In order to improve the last estimate after each time, $\Delta\vec{h}$ was added to $\vec{h}$. This process continued until all $\Delta\vec{h}$ components were negligible compared with $\vec{h}$. In the present work, the whole iteration procedure demanded up to 48 h in a CDC3600 IBM computer machine depending on the accuracy needed for the coefficients.

4. Results and discussion

4.1. Heat transfer coefficient at metal–mould interfaces

After casting, the cylindrical samples were divided into two equal parts through their longitudinal axes. One part was etched chemically to reveal its dendritic macrostructure. In experiments Eq-Inoc and Col-Inoc, the dendrite structure was fully equiaxed; while in experiments Eq-NoInoc and Col-NoInoc, a columnar dendritic structure 20 and 40 mm long, respectively, as found adjacent to the metal–copper base interface. Columnar dendrite trunks were approximately parallel to the longitudinal axis of the cylindrical sample.

The heat transfer coefficient between metal and copper base calculated as explained before is shown in Figs. 2 and 3. The temperature field generated by the heat transfer mathematical model employing the calculated heat transfer coefficients was compared with the measured temperatures. A very good agreement was observed between them, as can be seen by the curves shown in Fig. 4.

The following heat transfer steps and thermal resistance components, given between parentheses, can be identified in the experiments where a coated massive base was employed to extract heat (experiments Eq-Inoc and Eq-NoInoc) [3]:

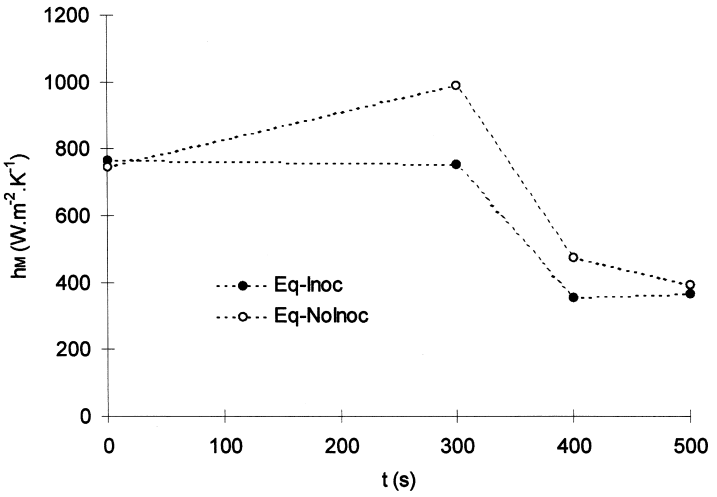

Fig. 2. Heat transfer coefficient between metal and massive copper base as a function of time for experiments Eq-Inoc and Eq-NoInoc.

- heat transfer across the metal–ceramic coating interface ($1/h_{MR}$);
- heat conduction through the porous ceramic coating ($\Delta x_c/K_c$);
- heat transfer across the coating–copper base interface ($1/h_{MB}$).

The global thermal resistance between metal surface and massive base surface is:

$$\frac{1}{h_M} = \frac{1}{h_{MR}} + \frac{\Delta x_c}{K_c} + \frac{1}{h_{MB}} \tag{12}$$

Chiesa [3] has measured the heat transfer coefficient between liquid metals and coated metallic moulds and reported values from 510 to 1030 W m^{-2} K^{-1} for coating thicknesses in the range from 83–392 μm. It can be seen in Fig. 2 that, at the beginning of simulation, when some liquid metal probably exists, the heat transfer coefficient is in the range mentioned above.

Heat is transferred across the metal–coating interface by three possible mechanisms: convection and conduction in the gas filling the gap at the metal–ceramic coating interface; radiation across this gap and

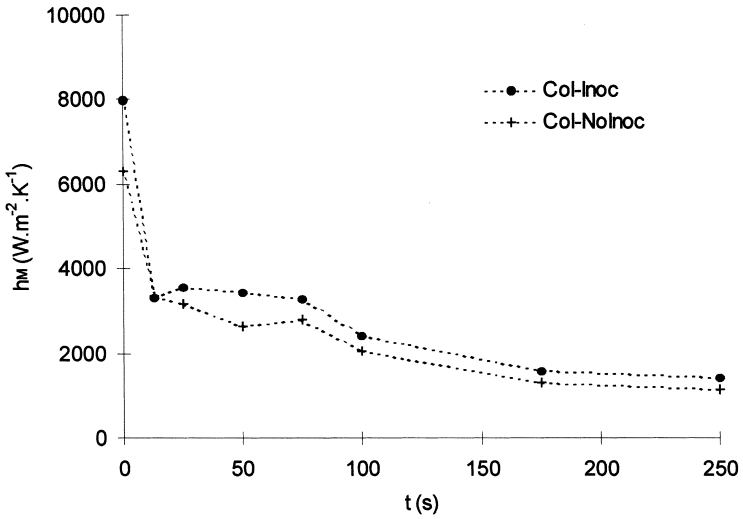

Fig. 3. Heat transfer coefficient between metal and water-cooled base as a function of time for experiments Col-Inoc and Col-NoInoc.

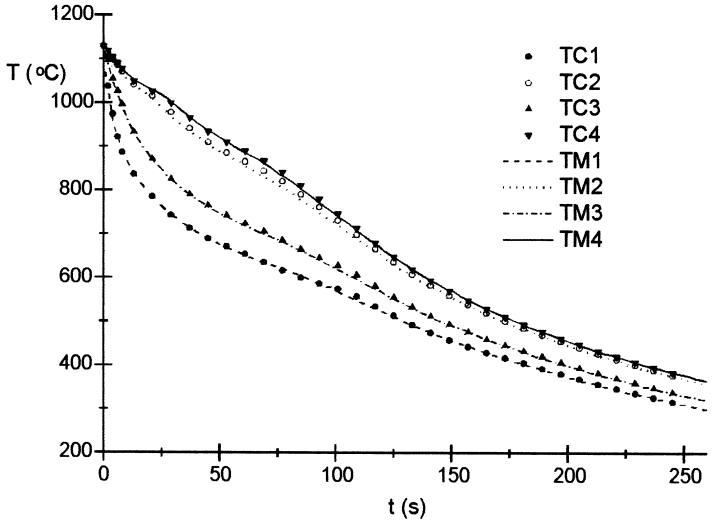

Fig. 4. Temperatures calculated (TC) by the heat transfer model are compared with temperatures measured (TM) in experiment Col-NoInoc.

conduction through contact points. Calculating the magnitude of radiation heat flux between metal and coating surfaces can indicate the importance of heat transfer by radiation. In order to simplify calculations, a continuous and uniform gap was assumed to exist between two parallel planes representing both metal and coating surfaces. The radiation heat flux can be computed by the following equation [1]:

$$qr = \frac{\sigma\left(T_{\mathrm{Ms}}^4 - T_{\mathrm{cs}}^4\right)}{(1/\varepsilon_{\mathrm{M}}) + (1/\varepsilon_{\mathrm{c}}) - 1} \tag{13}$$

The temperature at the coating surface T_{cs} was assumed to be much smaller than T_{Ms} and was neglected. The possible error introduced by this approximation overestimates the radiation heat flux. The metal surface temperature, T_{Ms}, was computed by the

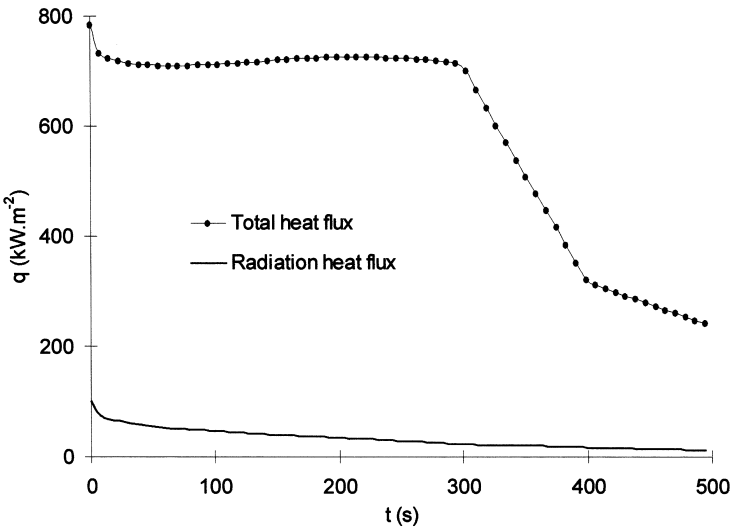

Fig. 5. Total heat flux in experiment Eq-NoInoc and its component due to radiation across metal–ceramic coating interface.

heat transfer mathematical model after calculating the heat transfer coefficients. Results of radiation and total heat flux across the same interface are shown in Fig. 5.

It can be seen that the radiation heat flux across metal–coating interface is negligible. Consequently, heat transfer by radiation cannot be the prevailing mechanism. Heat conduction and convection across the gas filling the gap and conduction through contact points must arise as the most important mechanisms. This might be explained by the fact that a clearance gap cannot have appeared at the interface, since it is subjected to the pressure of the cylinder weight.

Fig. 5 also shows that there is an abrupt fall of the total heat flux between 300 and 400 s, which can be attributed to the formation of a non-conforming solid skin, preventing intimate contact between metal and coating surfaces.

An analysis of the importance of the thermal resistance across the porous ceramic coating was made by calculating $\Delta x_c/K_c$, where K_c was estimated to be 1.5 W m^{-1} K^{-1}, according to Chiesa [3], and after assuming a mullite based coating with a void fraction of 0.6. The resulting thermal resistance was 5×10^{-4} W $^{-1}$ m^2 K, which can be compared with the total thermal resistance ($1/h_M$) calculated from Fig. 2. This total thermal resistance varied from approximately 13–25 $\times 10^{-4}$ W^{-1} m^2 K in experiment Eq-NoInoc. This shows that the ceramic coating offers a considerable resistance to heat extraction in metallic moulds when no clearance gap is formed.

Considering that the thermal resistance at coating–copper base interface ($1/h_{MB}$) cannot have changed significantly during experiment, the observed increase in the calculated total thermal resistance can only be the result of a rise in the metal–coating interface thermal resistance. This rise was approximately 12×10^{-4} W^{-1} m^2 K, which should not be overlooked, for it can represent as much as half the total resistance after 350 s. Chiesa [3] has also realised the importance of the thermal resistance at metal–coating interface, since, in his experiments, changes in coating roughness caused major variations of the global heat transfer coefficient when the metal was still liquid.

A similar analysis can be made about the results of experiment Eq-Inoc, thus it will not be repeated here.

As regards experiments Col-Inoc and Col-NoInoc, the following heat transfer steps and thermal resistances can be described:

- heat transfer across metal–water-cooled base interface ($1/h_{MC}$);
- heat conduction through the wall of the water-cooled base ($\Delta x_L/K_L$);
- heat transfer between the inner surface of the water-cooled base and the cooling water ($1/h_{MW}$).

The total thermal resistance is given by:

$$\frac{1}{h_M} = \frac{1}{h_{MC}} + \frac{\Delta x_L}{K_L} + \frac{1}{h_{MW}} \tag{14}$$

The component h_{MW} is approximately 21 kW m^{-2} K^{-1}, which was derived from standard relationships [12]. $K_L/\Delta x_L$ can be calculated, where K_L is the thermal conductivity of electrolytic copper (mould material) and Δx_L is the mould wall thickness (5×10^{-3} m), resulting in 79,600 kW m^{-2} K^{-1}. An analysis of these values and $1/h_M$ from Fig. 3 reveals that the most considerable thermal resistance can only be that at the metal–copper base interface ($1/h_{MC}$), all other thermal resistances ($1/h_{MW}$ and $\Delta x_L/K_L$) being negligible. Therefore, the heat transfer coefficient at metal–copper base interface (h_{MC}) can be represented, to a good approximation, by the global heat transfer coefficient between metal and cooling water (h_M), given in Fig. 3.

The behaviour of h_M is in good agreement with that summarised by Sharma and Krishnan [2]. Initially, high values are present owing to the intimate contact between liquid metal and the copper base surface. As the metal surface temperature decreases, a solid metal skin is formed preventing a conforming contact. This results in a decrease in the heat transfer coefficient. A steady state is finally reached when the growth of the solid metal layer no longer affects the gap at the interface and when the pressure applied at the interface does not change with time. This steady state value was nearly 1400 W m $^{-2}$ K^{-1}, which is comparable to 1000 W m^{-2} K^{-1}, a value reported by Spitzer [6], Ho and Pehlke [1], and Bamberger et al. [13].

The total and radiation heat fluxes were calculated in experiment Col-NoInoc by the same approach as that used in the massive base experiment described earlier. The average radiation heat flux was approximately 7 kW m^{-2}, which can be neglected when compared with the total heat flux shown by Fig. 6. Thus, the radiation heat flux component must also have a minor importance in the heat extraction process for the water-cooled base experiments. This might be an evidence that the heat conduction and convection through the gas, and conduction at contact points, are prevailing mechanisms to transfer heat across the metal–water-cooled base interface. An attempt was made to evaluate the importance of heat conduction across the air gap at the interface by assuming a continuous gap to exist between two ideal planes located at the metal and mould surfaces. The width of this ideal gap (Δx_g) was calculated considering that the total heat flux shown in Fig. 6 was the sole result of conduction in the air trapped there. After using the relationship $\Delta x_g = K_g/h_M$, where K_g is air thermal conductivity (0.05 W m^{-1} K^{-1}), calculation results are given in Fig. 6.

In experiment Col-NoInoc, the roughness of the

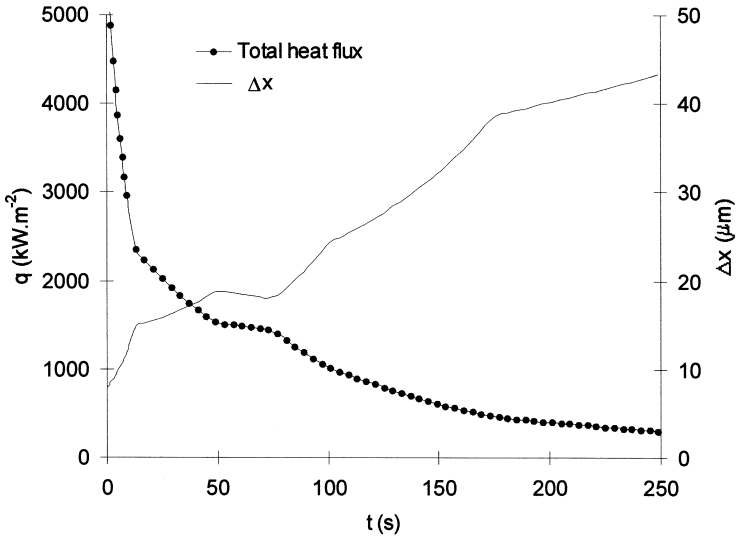

Fig. 6. Total heat flux (q) and ideal gap (Δx) at metal–water-cooled mould interface as function of time for experiment Col-NoInoc.

cylindrical sample at the bottom surface in contact with the copper base was measured by a rugosimetre yielding[4] $Ra = 2.98$ μm, $R_z = 16.4$ μm and $Ry = 27$ μm. If one assumes that the roughness at the mould surface is approximately the same as that at the casting surface previously in contact, and if R_z is used as the individual contribution of casting and mould surface roughness to the gap formed between contact points, a total gap of 32.8 μm is predicted. This gap is near the final gap size shown in Fig. 6. This might suggest that the main mechanism of heat transfer at the metal–water cooled mould interface is conduction through the air gap surrounding the contact points rather than conduction through these points.

It can be seen from Figs. 2 and 3 that the heat transfer coefficients in experiments Col-Inoc and Col-NoInoc are greater than those in experiments Eq-Inoc and Eq-NoInoc. This might be the result of the thermal insulating ceramic layer present at the latter experiments, which was previously seen to be one of the considerable thermal resistances to heat extraction.

Comparing the heat transfer coefficient of experiment Eq-Inoc with that of Eq-NoInoc and the heat transfer coefficient of Col-Inoc with that of Col-NoInoc, it seems reasonable to conclude that the inoculation treatment had no significant effect on these coefficients. The variations observed might as well be the result of random experimental errors.

4.2. Sensitivity analysis

The main idea of sensitivity coefficients in the IHCP is to have a comparative number on how sensitive thermocouples are to the heat transfer coefficient [4]. If the sensitivity coefficient of a certain thermocouple is too low, it will be difficult to calculate heat transfer coefficients by the inverse solution technique from its response. Experimental errors might affect this measurement as much as a real variation in the heat transfer coefficient. Consequently, it would not be possible to separate the effects, leading to very inaccurate results.

The sensitivity coefficient ($XhiTC$) to a specific component of the heat transfer coefficient h_i was calculated for a thermocouple, TC, placed at co-ordinates (r, z) and time t by:

$$\frac{\partial TC}{\partial h_i}(r,z,t) = XhiTC(r,z,t) \approx \frac{TC(r,z,t,h_1,\ldots,h_i+\varepsilon h_i,\ldots,h_n) - TC(r,z,t,h_1,\ldots,h_i,\ldots,h_n)}{\varepsilon h_i} \quad (15)$$

where $\varepsilon = 0.001$. Thus, the sensitivity coefficient ($XhiTC$) of each component of h_M and h_m for thermocouples TM1–TM4 can be calculated as a function of time.

[4] $Ra = 1/L \int_0^L |y|\,dL$; $R_z = \sum_{i=1}^{n} z_i$; Ry = distance between the highest peak and the deepest valley along the surface microprofile measured by a rugosimetre. L is the sampling length; y is the vertical position relative to the mean line; z_i is the distance between a peak and its adjacent valley and n is the number of peaks analysed. Three microprofiles of 7.5 mm sampling length were measured and the reported values are average ones.

It was observed that the sensitivity coefficients of all h_M components for thermocouple TM1 are three times as high as the sensitivity coefficients for TM4. Therefore, a more efficient experimental approach could be adopted by placing thermocouple TM4 at the same vertical position as TM1, increasing the accuracy of the heat transfer coefficient obtained.

The heat transfer coefficient at the metal–insulating sleeve interface (h_m) was also calculated by the whole domain method and its value varied widely in the range of 200–5000 W m^{-2} K^{-1} from one experiment to another. In addition to it, the sensitivity coefficients of h_m for all thermocouples in all experiments were calculated and were seen to be approximately two orders of magnitude smaller than the sensitivity coefficients of each h_M component. Therefore, h_m should be much more affected by experimental errors, explaining the wide spread of h_m values observed.

Although the meaning of sensitivity coefficients has been thoroughly explained in the literature [4], never has a quantitative analysis been put forward before. This will be attempted below.

Since the calculated heat transfer coefficient components depend on all temperature measurements in each experiment, the following functional form can be written:

$$h_i = h_i\big(TM_{1,1}, TM_{1,2}, \ldots, TM_{1,p}, TM_{2,1}, TM_{2,2}, \ldots, TM_{k,v}, \ldots, TM_{q,1}, \ldots, TM_{q,p}\big) \tag{16}$$

Approximating the above functional by a first-order Taylor series, one has:

$$\Delta h_i \approx \sum_{k=1}^{q}\sum_{v=1}^{p}\left[\left(\frac{\partial h_i}{\partial TM}\right)_{k,v}\Delta TM_{k,v}\right] \tag{17}$$

Each $\Delta TM_{k,v}$ might be considered as an experimental error in the temperature measured by a thermocouple located at (r_k, z_k) at time t_v. Δh_i is the total error propagated to the heat transfer coefficient component h_i. An average value for the derivatives in Eq. (17) can be defined as:

$$\Delta h_i = \overline{\frac{\partial h_i}{\partial TM}}\sum_{k=1}^{q}\sum_{v=1}^{p}\Delta TM_{k,v} \tag{18}$$

The heat transfer mathematical model can be used to estimate the above average value as follows:

$$\overline{\frac{\partial h_i}{\partial TM}} \approx \overline{\frac{\partial h_i}{\partial TC}} = \frac{\Delta h_i}{\sum_{k=1}^{q}\sum_{v=1}^{p}\Delta TC_{k,v}} \tag{19}$$

where $\Delta TC_{k,v}$ can be computed by the mathematical model as shown below:

$$\Delta TC_{k,v} \approx \left(\frac{\partial TC}{\partial h_i}\right)_{k,v}\Delta h_i \tag{20}$$

Defining $\Delta h_i = 1.0$ W m^{-2} K^{-1} and using Eqs. (15), (19) and (20), the following relation is derived:

$$\overline{\frac{\partial h_i}{\partial TM}} \approx \overline{\frac{\partial h_i}{\partial TC}} \approx \frac{1}{\sum_{k=1}^{q}\sum_{v=1}^{p} XhiTC_{k,v}} \tag{21}$$

where $XhiTC_{k,v}$ can be easily given by the heat transfer mathematical model and the right side of Eq. (15). Eq. (21) shows that the sensitivity of a certain heat transfer coefficient component to temperature errors can be diminished by including more temperature measurements of one thermocouple or adding more thermocouples to the system.

The analysis of a simple problem by the above treatment can give a better insight into the meaning of Eq. (21). Considering the application of Eq. (11) for a problem where h has only one component, namely h, the following equation is arrived at:

$$h = h^* + \frac{\sum_{k=1}^{q}\sum_{v=1}^{p}\big[TM_{k,v} - TC_{k,v}(h^*)\big]\mathrm{d}TC_{k,v}/\mathrm{d}h\,|_{h^*}}{\sum_{k=1}^{q}\sum_{v=1}^{p}\big(\mathrm{d}TC_{k,v}/\mathrm{d}h\,|_{h^*}\big)^2} \tag{22}$$

where h^* is a tentative value of the heat transfer coefficient sufficiently close to the actual value h. Assuming that each measured temperature $TM_{k,v}$ is affected by an experimental error $\Delta TM_{k,v}$, the following equation can be written:

$$\Delta h = \sum_{k=1}^{q}\sum_{v=1}^{p}\left[\Delta TM_{k,v}\frac{\mathrm{d}TC_{k,v}/\mathrm{d}h\,|_{h^*}}{\sum_{k=1}^{q}\sum_{v=1}^{p}\big(\mathrm{d}TC_{k,v}/\mathrm{d}h\,|_{h^*}\big)^2}\right] \tag{23}$$

where Δh is now the error in the heat transfer coefficient owing to an error in the measured temperatures. Comparing Eq. (23) with Eq. (17) results in the relationship given below:

$$\left(\frac{\partial h}{\partial TM}\right)_{k,v} = \frac{\mathrm{d}TC_{k,v}/\mathrm{d}h\,|_{h^*}}{\sum_{k=1}^{q}\sum_{v=1}^{p}\big(\mathrm{d}TC_{k,v}/\mathrm{d}h\,|_{h^*}\big)^2} \tag{24}$$

This equation shows that when another temperature measurement, e.g. $TM_{q+1,p}$, is included in the calculation of h, a positive term is added to the denominator. This reduces all $(\partial h/\partial TM)_k$, v coefficients present in Eq. (17). Therefore, the error of each temperature measurement propagated to h is decreased, which is in accordance with the analysis made before.

Nevertheless, when a new temperature measurement is included, Eq. (17) also shows that a term proportional to $\Delta TM_{q+1,\,p}$ should be added to the expansion. A relatively large error associated with the new temperature measurement $TM_{q+1,\,p}$ might offset the benefit shown by Eq. (24) or even increase the error in h.

Let a certain temperature measurement error be present, causing an error in h. If this incorrect value of h was used by the heat transfer mathematical model to calculate the temperature in a place with no thermocouple, a difference between the calculated and the actual temperature, $TC_{q+1,\,p} - T_{q+1,\,p}$, would possibly exist. Assume now that a thermocouple was placed exactly at the position where the calculated temperature was obtained. If an error of the same magnitude as $TC_{q+1,\,p} - T_{q+1,\,p}$ existed in the temperature measurement, it is clear that this should not change the error in h. Therefore, the following equation can be written:

$$\begin{aligned}\Delta h &= \sum_{k=1}^{q}\sum_{v=1}^{p}\left[\left(\frac{\partial h}{\partial TM}\right)_{k,\,v}\Delta TM_{k,\,v}\right] \\ &= \sum_{k=1}^{q}\sum_{v=1}^{p}\left[\left(\frac{\partial \hat{h}}{\partial TM}\right)_{k,\,v}\Delta TM_{k,\,v}\right] \\ &\quad + \left(\frac{\partial \hat{h}}{\partial TM}\right)_{q+1,\,p}\Delta TM_{q+1,\,p}\end{aligned} \tag{25}$$

where $\hat{h}$ is a functional similar to that given by Eq. (16) for h, but including $TM_{q+1,\,p}$ in the list of arguments. Eq. (25) shows that if all coefficients of ΔTM and ΔTM itself are either positive or negative, then:

$$\left(\frac{\partial \hat{h}}{\partial TM}\right)_{k,\,v} < \left(\frac{\partial h}{\partial TM}\right)_{k,\,v} \tag{26}$$

since Δh is constant. Thus, one concludes, again, that h becomes less sensitive to the error associated with each temperature measurement when a new thermocouple measurement is included in the calculations.

A quantitative analysis can be used to estimate the error in each component of $\vec{h}$ in the present work experiments. After knowing $\overline{\partial h_i/\partial TM}$, the error in h_i, namely Δh_i, can be calculated for any experimental error $\Delta TM_{k,\,v}$ with the help of Eq. (18). Assuming that a systematic error of 1°C occurred in all 500 temperature measurements recorded from one thermocouple during experiment Col-NoInoc, the following error is expected to propagate to the first component of h_{M}:

$$\begin{aligned}\Delta h_1 &\approx \overline{\frac{\partial h_1}{\partial TC}} \times 1 \times 500 = 0.42 \times 1 \times 500 \\ &= 210\ \mathrm{W\ m^{-2}\ K^{-1}}\end{aligned} \tag{27}$$

Table 2
Heat transfer coefficient error (Δh_i) for all h_{M} components and h_{m} in experiment Col-NoInoc

i	Δh_i (W m^{-2} K^{-1})	$\overline{\frac{\partial h_i}{\partial TM}}$ (W m^{-2} K^{-2})	100% ($\Delta h_i/h_i$)
1	209	0.42	3.3
2	211	0.42	6.3
3	77	0.16	2.4
4	31	0.06	1.2
5	48	0.10	1.7
6	21	0.04	1.0
7	15	0.03	1.2
8	58	0.12	5.0
m	2947	5.89	54.8

In this work, systematic errors might be expected from calibration errors of commercial thermocouples, which might reach up to 10°C at high temperatures. Moreover, the presence of a ceramic coating to protect thermocouple junctions might cause a temperature measurement lag, which may also be a source of systematic errors. Error propagation was also calculated for the other components of h_{M} and h_{m} and is shown in Table 2. It can be seen that the error in h_{m} is much greater than that in h_{M} components, supporting the previous idea of a very inaccurate h_{m} due to its smaller sensitivity coefficient. Δh_{m} can amount to as much as 50% of h_{m}, whereas Δh for h_{M} components is always smaller than approximately 5%, as given by Table 2. The preceding analysis can be extended to assess the effect of errors associated with certain parameters, e.g. thermocouple position or temperature measurement lag. Application of the chain rule to Eq. (18) results in:

$$\begin{aligned}\Delta h_i = \overline{\frac{\partial h_i}{\partial TM}}\sum_{k=1}^{q}\sum_{v=1}^{p}\Bigg[&\frac{\partial TM_{k,\,v}}{\partial r}\Delta r_k + \frac{\partial TM_{k,\,v}}{\partial z}\Delta z_k \\ &+ \frac{\partial TM_{k,\,v}}{\partial t}\Delta t_v\Bigg]\end{aligned} \tag{28}$$

where all partial derivatives are calculated at co-ordinates (r_k, z_k,) and time t_v. After defining average values for the partial derivatives by expressions similar to Eq. (19), the following relation is derived from Eq. (28):

$$\begin{aligned}\Delta h_i = \overline{\frac{\partial h_i}{\partial TM}}\Bigg(&p\overline{\frac{\partial TM}{\partial r}}\sum_{k=1}^{q}\Delta r_k + p\overline{\frac{\partial TM}{\partial z}}\sum_{k=1}^{q}\Delta z_k \\ &+ q\overline{\frac{\partial TM}{\partial t}}\sum_{v=1}^{p}\Delta t_v\Bigg)\end{aligned} \tag{29}$$

where $\overline{\frac{\partial TM}{\partial r}}$ and $\overline{\frac{\partial TM}{\partial z}}$ are the average temperature variation in the radial and longitudinal directions, respectively, and $\overline{\frac{\partial TM}{\partial t}}$ is the average cooling rate.

In the present work experiments, the maximum temperature variation in the longitudinal direction observed around TM1, for experimental condition Col-NoInoc, was 133 K cm^{-1}. Consequently, an error of 1 mm in determining the location of that thermocouple along the longitudinal direction would cause an error of 13 K in its temperature. According to the analysis made previously, this might bring about an error of approximately 40% to the first component of h_M. On the other hand, for the region neighbouring TM2, where the longitudinal temperature variation is around 87 K cm^{-1}, the error would decrease to 26%. It was previously seen that the closer the thermocouple is to the copper base, the higher the sensitivity coefficient becomes. However, the error propagated to h_M might increase if its location is not determined accurately. In this case, it is preferable to place thermocouples farther from the copper base.

This investigation is just a first attempt to make a more efficient use of sensitivity coefficients. A more elaborate analysis is expected, however, if more detailed information is to be withdrawn from them.

5. Conclusions

The following conclusions can be drawn from the present work:

1. The complete domain estimation can give heat transfer coefficient values between metal and water-cooled or massive copper base which are in good agreement with the published data.
2. The heat transfer coefficient values at metal–insulating sleeve interface calculated by the whole domain estimation are widely spread compared with its absolute value.
3. An approximate analysis of the heat transfer between the cast alloy and the massive copper base shows that the thermal resistance at the metal–ceramic coating interface can represent nearly half of the total thermal resistance for heat extraction in the system.
4. Approximate calculations have shown that the thermal resistance between metal surface and water cooled base surface is the most important one for heat extraction in this system.
5. A quantitative analysis of sensitivity coefficients gave results that can explain the wide spread observed in the heat transfer coefficient at the metal–insulating sleeve interface (h_m).
6. Inoculation of the melt has not caused a significant variation of the heat transfer coefficient between the cast alloy and the copper bases.

Acknowledgements

The authors wish to thank for the financial support to this work given by Fundação de Amparo à Pesquisa do Estado de São Paulo (FAPESP) and Coordenação de Aperfeiçoamento de Pessoal de Nível Superior (CAPES).

References

[1] K. Ho, R.D. Pehlke, Metal–mold interfacial heat transfer, Metallurgical Transactions 16B (1985) 585–594.
[2] D.G.R. Sharma, M. Krishnan, Simulation of heat transfer at casting metal–mold interface, Transactions of The American Foundrymen's Society 99 (1991) 429–438.
[3] F. Chiesa, Measurement of the thermal conductance at the mold/metal interface of permanent molds, Transactions of The American Foundrymen's Society 98 (1990) 193–200.
[4] J.V. Beck, B. Blackwell, C.R. St. Clair Jr, in: Inverse Heat Conduction, 1st ed., Wiley, New York, 1985, p. 119.
[5] I. Frank, An application of least squares method to the solution of the inverse problem of heat conduction, Journal of Heat Transfer 85 (1963) 378–379.
[6] K.H. Spitzer, Investigation of heat transfer between metal and water cooled belt using a least square method, International Journal of Heat and Mass Transfer 34 (1991) 1969–1974.
[7] M.A. Martorano, Efeitos de algumas variáveis de processo na microssegregação da liga Cu–8%Sn (Translation: Effects of some processing variables on the microsegregation of Cu–8%Sn alloy), PhD thesis, University of São Paulo, Sao Paulo, SP, 1998 (in Portuguese).
[8] N. Shamsundar, E. Rooz, Numerical methods for moving boundary problems, in: W.J. Minkowycz, E.M. Sparrow, G.E. Schneider, R.H. Pletcher (Eds.), Handbook of Numerical Heat Transfer, 1st ed., Wiley, New York, 1988, pp. 747–786.
[9] H.D. Brody, M.C. Flemings, Solute redistribution in dendritic solidification, Transactions of The Metallurgical Society of AIME 236 (1966) 615–624.
[10] W.T. Clyne, W. Kurz, Solute redistribution during solidification with rapid solid state diffusion, Metallurgical Transactions A 12A (1981) 965–970.
[11] R.W. Daniels, An Introduction to Numerical Methods and Optimization Techniques, Elsevier/North-Holland, New York, 1978, pp. 237–264.
[12] G.H. Geiger, D.R. Poirier, Transport Phenomena in Materials Processing, 1st ed., Mineral Metals and Materials Society, Warrendale, PA, 1992, pp. 247–279.
[13] M. Bamberger, B.Z. Weiss, M.M. Stupel, Heat flow and dendritic arm spacing in chill-cast Al–Si alloys, Materials Science and Technology 3 (1987) 49–56.